PCCP

Bond Dissociation Energies of Low-Valent Lanthanide Hydroxides: Lower Limits from Ion-Molecule Reactions and Comparisons with Fluorides

Journal:	*Physical Chemistry Chemical Physics*
Manuscript ID	CP-ART-03-2021-001362.R1
Article Type:	Paper
Date Submitted by the Author:	26-Apr-2021

Complete List of Authors:	Parker, Mariah; Lawrence Berkeley National Laboratory, Chemical Sciences Division Jian, Jiwen; Zhejiang Normal University Gibson, John; Lawrence Berkeley National Laboratory, Chemical Sciences Division

Bond Dissociation Energies of Low-Valent Lanthanide Hydroxides: Lower Limits from Ion-Molecule Reactions and Comparisons with Fluorides

Mariah L. Parker, Jiwen Jian[†] and John K. Gibson[*]

Chemical Sciences Division, Lawrence Berkeley National Laboratory, Berkeley, CA 94720 USA

[*]Corresponding author email: jkgibson@lbl.gov

[†]Present address: Hangzhou Institute of Advanced Studies, Zhejiang Normal University, 1108 Gengwen Road, Hangzhou, Zhejiang, 311231, China.

Keywords

Bond dissociation energy; Lanthanide hydroxide; Lanthanide fluoride; Gas-phase reaction

Abstract

Despite that bond dissociation energies (*BDEs*) are among the most fundamental and relevant chemical properties they remain poorly characterized for most elementary lanthanide hydroxides and halides. Lanthanide ions Ln^+ = Eu^+, Tm^+ and Yb^+ are here shown to react with H_2O to yield hydroxides $LnOH^+$. Under low-energy conditions such reactions must be exothermic, which implies a lower limit of 499 kJ/mol for the Ln^+-OH *BDEs*. This limit is significantly higher than previously reported for $YbOH^+$ and is unexpectedly similar to the *BDE* for Yb^+-F. To explain this apparent anomaly, it is considered feasible that the inefficient hydrolysis reactions observed here in a quadrupole ion trap mass spectrometer may actually be endothermic. More definitive and broad-based evaluations and comparisons require additional and more reliable *BDEs* and ionization energies for key lanthanide molecules, and/or energies for ligand-exchange reactions like LnF + OH ↔ LnOH + F. The hydroxide results motivated an assessment of currently available lanthanide monohalide *BDEs*. Among several intriguing relationships is the distinctively higher *BDE* for neutral LuF versus cationic LuF^+, though quantifying this comparison awaits a more accurate value for the anomalously high ionization energy of LuF.

Introduction

Metal hydroxides are ubiquitous in condensed phase processes ranging from commonplace rusting to advanced energy storage and conversion.[1-3] In the gas phase they are key constituents in phenomena such as high-temperature corrosion and material transport.[4, 5] Small gas-phase metal hydroxide molecules furthermore provide a basis to elucidate the essential nature of underlying bonding interactions, and reactivity relevant to more complex systems and practical applications.[6] Electropositive lanthanides are particularly prone to solution hydrolysis,[7-9] with the resulting hydroxides commonly employed in catalysis, optics and electronics.[10-13] Understanding hydroxides is often advanced by modeling them as pseudo-halides, particularly as isoelectronic fluorides.[14-18] Similar electronic properties of YbF and YbOH, for example, designate both as prime candidates to evaluate the electric dipole moment of the electron.[19, 20] The bond between a lanthanide (Ln) and halide or hydroxide (X) is often effectively modeled as ionic—i.e., LnX represented as $(Ln^+)(X^-)$—with perturbations introduced by parameters such as polarization and ligand fields.[17, 18, 21-23] Although fully ionic $(Ln^+)(X^-)$ is sometimes a useful approximation, deviations due to bond covalency can significantly affect properties.[24-26]

Among the most fundamental characteristics of a molecule is the bond dissociation energy (*BDE*), as given for LnX^+ by reaction (1), which is for the cation rather than neutral LnX mainly because ions are amenable to manipulation by electric and magnetic fields in common experimental techniques like mass spectrometry. The *BDEs* of neutral LnX and cation LnX^+ are related through ionization energies (IEs) by equation (2). Whereas molecular properties such as effective electric field can often be accurately computed,[19, 20] computation of *BDEs* is often complicated by large disparities between electronic structures of bound LnX^+ versus the constituent fragments Ln^+ and X.[27, 28] Because the formal lanthanide oxidation states are $Ln^{(I)}$ and $Ln^{(II)}$ in LnX and LnX^+, respectively, the *BDEs* reflect relative stabilities of these low valence states towards further reduction. Formation of LnX^+ can occur by reaction (3), where X-atom donor RX may be an organic (C_mH_nX), a hydrogen halide (HX), or water in the specific case of reaction (3′). Under low-energy conditions, occurrence of reaction (3) or (3′) requires that it is exothermic (or thermoneutral), with $BDE[Ln^+\text{-}X] \geq BDE[R\text{-}X]$.

(1) $Ln^+ + X \rightarrow LnX^+$ $\Delta E_1 = -BDE[Ln^+\text{-}X]$

(2) $BDE[Ln^+\text{-}X] - BDE[Ln\text{-}X] = IE[Ln] - IE[LnX]$

(3) $Ln^+ + RX \rightarrow LnX^+ + R$ $\Delta E_3 = BDE[R\text{-}X] - BDE[Ln^+\text{-}X]$

(3′) $Ln^+ + H_2O \rightarrow LnOH^+ + H$ $\Delta E_{3'} = BDE[H\text{-}OH] - BDE[Ln^+\text{-}OH]$

Reaction (3′) was previously studied for all lanthanides except Pm by Bohme et al. using inductively coupled plasma (ICP) as the metal ion source and selected-ion flow-tube mass spectrometry (SIFT-MS) to study kinetics.[29] Observation of reaction (3′) for Ln = La, Pr and Yb established $BDE[Ln^+\text{-}OH] \geq BDE[H\text{-}OH]$ (499 kJ/mol[30]). This result for $YbOH^+$ was notable as reaction (3) was not previously observed for Ln = Yb with alcohols (ROH) that have *BDE*[R-OH] below 499 kJ/mol, such that those reactions should also be exothermic.[31, 32] Reaction (3′) was not reported for Ln = Eu or Tm by Bohme et al.,[29] indicating either a thermodynamic constraint due to $BDE[Ln^+\text{-}OH] < 499$ kJ/mol, or kinetic hindrance.

In the present work, reaction (3′) was re-examined for Ln = Eu, Tm and Yb using electrospray ionization (ESI) to generate Ln^+, and quadrupole ion trap mass spectrometry (QIT-MS) to study reactivity. It was found that reaction (3′) occurs, albeit inefficiently, for all three Ln. Assuming that the QIT reactions are for nearly thermal ions, the results would imply *BDE*[Ln^+-OH] ≥ 499 kJ/mol, which is higher than previously reported values for Ln = Eu and Yb. Specifically, high-temperature equilibrium studies yielded *BDE*[Yb-OH] values of 377±8 kJ/mol[33] and 322±12 kJ/mol.[34] Using IE[YbOH] = 583±5 kJ/mol[35] and IE[Yb] = 602.6 kJ/mol,[30] these *BDEs* for neutral YbOH provide the following cation values via equation (2): *BDE*[Yb^+-OH] = 397 kJ/mol and 342 kJ/mol; both of these are below the tentative minimum of 499 kJ/mol established here from reaction (3′). Also, the reaction (3′) lower limit for $EuOH^+$ conflicts with previously reported *BDE*[Eu^+-OH] = 423±7 kJ/mol.[36] Given these disparities between reported *BDE*[Ln^+-OH] and lower limits from reaction (3′) under presumed low-energy conditions, corresponding trends for *BDE*[Ln^+-F] and *BDE*[Ln^+-Cl] are considered for comparison. A striking result is the possible similarity between *BDE*[Yb^+-OH] and *BDE*[Yb^+-F], though this comparison is only tentative given different results for reaction (3′) using different experimental approaches, as discussed below. The present results and assessment highlight uncertainties in *BDEs* for the most fundamental lanthanide halide and hydroxide molecules, hopefully encouraging further experiments and computations on these systems.

Experimental Methods

Experiments were performed with an Agilent 6340 electrospray ionization quadrupole ion trap mass spectrometer (ESI-QIT/MS) described previously.[37] The ESI solutions were 0.2 mM $EuCl_3$, $TmCl_3$ or $YbCl_3$ prepared in ethanol without rigorously excluding water (<10% H_2O). Solutions were injected into the ESI capillary via a syringe pump at 75 μL/h. Mass spectra were acquired in the positive ion accumulation and detection mode using the following instrumental parameters: nebulizer gas pressure, 12 psi; capillary voltage and current, -4500 V and 1 nA; end plate voltage offset and current, -500 V and 50 nA; dry gas flow rate, 2.0 L/min; dry gas temperature, 325 C; capillary exit, 300.0 V; skimmer, 30.6 V; octopole 1 and 2 DC, 12.0 V and 0.0 V; octopole RF amplitude, 50.0 Vpp; lens 1 and 2, -15.0 V and -98.5 V; trap drive, 31.1. Minor adjustments were sometimes made to these parameters to obtain enhanced intensities of specific ions. Nitrogen gas was used for nebulization and drying in the ion transfer capillary. The background water pressure in the ion trap was estimated as ~10^{-6} Torr.[38, 39] As this water pressure can vary by up to a factor of two, the relative pressure was determined for each set of experiments from pseudo-first order kinetics for hydration of uranyl hydroxide: $UO_2(OH)^+ + H_2O \rightarrow UO_2(OH)(H_2O)^+$.[38] To allow for direct comparison of kinetics at different water pressures, reported rates are normalized to a fixed background water pressure, except when additional water was deliberately added to the ion trap. Ions isolated in the QIT are estimated to be at T ≈ 300 K,[40-42] an issue discussed below.

Results and Discussion

(i) Reactions of lanthanide ions Ln^+ with water

Bare ions Eu^+, Tm^+ and Yb^+ were produced by ESI. An isotope with a particular mass-to-charge ratio *m/z* was trapped in the QIT and exposed to background H_2O and O_2 for a variable reaction time, in some cases with additional H_2O added to the ion trap. Mass spectra acquired after the maximum accessible reaction time of 10 s are in Figure 1, where a $LnOH^+$ product peak indicates reaction (3′). Time-dependent decay plots such as in Figure 2 show pseudo-first order kinetics. Included in Figure 2 are typical kinetics for hydration of $UO_2(OH)^+$ for determining relative H_2O pressures. Kinetics data such as those in Figure 2 were generally more uncertain for Ln = Tm due to extremely low reaction efficiency and product abundances. Despite constraints due to low product intensities and some non-linearity, decay plots such as in Figure 2 suggest pseudo-first order reaction (3′).

The $UO_2(OH)^+$ ion used for the pressure calibration was obtained directly from ESI of a uranyl solution. In contrast to the reactivity reported here for bare Ln^+ with water, it was previously shown that the reaction of UO_2^+ with H_2O under low-energy conditions in a QIT results in adsorption to yield hydrate $UO_2(H_2O)^+$, rather than hydrolysis to yield hydroxide $UO_2(OH)^+$.[38] Gas-phase uranyl, UO_2^{2+}, has been synthesized by sequential reaction of bare dipositive U^{2+} with O_2.[43] The reaction of U^{2+} with H_2O has been reported to yield UOH^{2+} with fairly high efficiency ($k/k_{col} = 0.11$).[44] The primary UOH^{2+} product reacts with a second H_2O molecule via a charge-reduction process to produce UO^+ ($+H_3O^+$).

Kinetics for reaction (3′) are summarized in Table 1 along with previously reported SIFT results.[29] The present QIT rates are adjusted to a constant background water pressure. By assuming a QIT water pressure of roughly 10^{-6} Torr, estimates were also obtained for k'/k_{col} where k′ is the pseudo-first order rate constant and k_{col} is the collisional constant.[29] The SIFT experiments for Ln = Eu, Tm and Yb showed only Yb exhibited reaction (3′). The QIT experiments, however, show reaction (3′) occurs for all three Ln, albeit inefficiently. The order of reaction (3′) rates from QIT is $Eu^+ > Yb^+ > Tm^+$, whereas from SIFT it was $Yb^+ > Eu^+$ and Tm^+, with no reaction observed for the last two. Another discrepancy appears for the k'/k_{col} for Yb^+, which is estimated as ~100× lower from QIT versus SIFT. Although the QIT estimate for k'/k_{col} employs an approximate $P[H_2O] \approx 10^{-6}$ Torr, it is unlikely that the actual pressure is sufficiently low—about 10^{-8} Torr—to bring the QIT and SIFT results into accord. The $UO_2(OH)^+$ hydration kinetics in Figure 2d would correspond to a water pressure of $4x10^{-8}$ Torr if the hydration efficiency is 100% ($k'/k_{col} = 1$); as the actual efficiency is likely lower, the actual water pressure is likely correspondingly higher.

Despite discrepancies between the QIT and SIFT results, a conclusion from both is that reaction (3′) is inefficient for Eu^+, Tm^+ and Yb^+. However, a key revision due to the QIT results is that reaction (3′) occurs for all three, which would establish a lower limit of $BDE[Ln^+\text{-OH}] \geq BDE[\text{H-OH}]$ (499 kJ/mol) if the reactions occur under truly thermal conditions. This minimum for Yb^+ would be particularly significant given previous results noted above that indicate

BDE[Yb^+-OH] < 400 kJ/mol.[33-35] There is also a disparity between the tentative new minimum and the reported value of *BDE*[Eu^+-OH] ≈ 423 kJ/mol.[36] There does not appear to be a previous determination of *BDE*[Tm^+-OH] for comparison.

Bohme et al. qualified their Yb^+ SIFT kinetics for reaction (3′) by noting that the reported k'/k_{col} might have resulted from an electronically excited-state Yb^+ population of only 0.4%.[29] In contrast to high-energy ICP ion source in SIFT, the ESI source for QIT transfers ions from solution in a relatively low-energy process, with less potential for excitation. Kinetics plots such as in Figure 2c are not fully linear, which may reflect very low ion intensities, but possibly also deviations from true pseudo-first order kinetics. If the results do indicate nearly invariant pseudo-first order kinetics to at least 10 s, it would suggest that the reactivity is determined by ground-state Yb^+, and/or by extraordinarily long-lived excited-state Yb^+. A key point is that pseudo-first order kinetics attributable to a bimolecular ion-molecule reaction do not *per se* indicate thermal reactivity. Nor do such pseudo-first order kinetics necessarily indicate a sole reactant ion state, but rather that all of the reacting states exhibit similar kinetics. Although the SIFT kinetics might have reflected electronically excited-state Yb^+, the QIT results seem to suggest that reaction (3′) occurs for ground-state Yb^+ given the very long lifetime that would be required for an excited state of Yb^+ to provide the results. The persistence of reaction (3′) in the QIT for ions collisionally cooled for periods of several seconds similarly suggests that the reactivity is not due to a population of kinetically excited Yb^+ ions present at the start of the reaction period. However, as noted below it is feasible that a small fraction of the isolated Yb^+ ions in the QIT might undergo continuous kinetic excitation that could provide sufficient energy to enable significantly endothermic reactions.

Just as excited-state Yb^+ might enable an endothermic reaction, so too might kinetically excited ions. Isolation of ions in the QIT with a particular *m/z* occurs by ejection of all ions with other values of *m/z*. As the applied ejection voltage is not a step function, there may be off-resonance excitation of retained ions. Such excitation should be greater for smaller isolation widths, *Δm/z*, as the ejection voltage is applied closer to the *m/z* of retained ions. To evaluate potential effects of off-resonance excitation, rates were measured for isolation widths of *Δm/z* = 1 and 2. Results such as in Figure S4 show only minor rate changes for different *Δm/z*, indicating negligible effects of off-resonance ion excitation due to the isolation conditions.

The pressure and composition of background reactant gases in the QIT are not well controlled.[39] Constituents H_2O and O_2 are monitored by association reactions with $UO_2(OH)^+$ and UO_2^+.[38] Low concentrations of unidentified OH-donor background gases besides H_2O are feasible. To confirm that H_2O is the dominant OH-donor, additional water was added to the ion trap, with the pressure increase determined hydration of $UO_2(OH)^+$. Kinetics determined for reaction (3′), such as in Figure S5, demonstrate that the yield of $LnOH^+$ increases in parallel with increasing water pressure, confirming H_2O as the dominant OH-donor, i.e. reaction (3′).

Reaction (3′) for lanthanide cations was also previously studied by Fourier-transform ion cyclotron resonance mass spectrometry (FTICR-MS), with the results as reported in the PhD thesis of H. H. Cornhel.[45] It was there conveyed that reaction (3′) does not occur for Ln = Eu, Tm

or Yb, where non-reactivity for the first two of these three lanthanide ions is in accord with the similarly negative results from SIFT.[29] Both the previous SIFT and FTICR-MS studies conflict with the present QIT results that show reaction (3′) occurs for Eu and Tm. The overall uncertain state of affairs is exacerbated by differing discord for reaction (3′) for Ln = Yb, for which FTICR-MS showed non-reaction whereas both SIFT and QIT gave positive results for an inefficient reaction. As both the SIFT[29, 46-48] and FTICR-MS[31, 32, 49, 50] approaches are well-established for studying gas-phase metal ion chemistry under low energy conditions, it seems unwarranted to conclude that the results from both previous studies are necessarily invalidated by the present results, despite that ion trap techniques, including QIT-MS, have also been demonstrated as applicable for reactivity studies.[40, 51-53] Notwithstanding the experiments described above to substantiate that the inefficient QIT reactions were not due to hyperthermal conditions, disparities with other techniques suggest the possibility for an unidentified source of kinetic excitation in the QIT that could enable endothermic reactions. Whereas in the SIFT technique metal ion-molecule reactions take place under the influence of a DC voltage in a high-pressure ion drift tube,[47, 48] reactions studied in a QIT are for ions continuously subjected to RF voltages for trapping.[54] The mean ion temperature in a QIT has been estimated as ~300 K, and it is almost certainly less than 1000 K.[40-42] Using the relationship for kinetic energy, $KE = 3/2 \cdot k \cdot T$ where k is the Boltzmann constant ($k = 1.38\times10^{-23}$ J/K = 8.31 J/mol·K), a temperature of 1000 K corresponds to a kinetic energy of ~12.5 kJ/mol. To enable a reaction that is endothermic by ~50 kJ/mol would require an effective ion temperature of ~4000 K. Although it is implausible that the average ion temperature in the QIT is sufficiently high to support a reaction endothermic by significantly more than ~10 kJ/mol, only a small fraction of the ions would need to be momentarily excited to a sufficiently high effective temperature to account for inefficient processes such as reported here for reaction (3′). Regardless of the origins of the disparity between the observed reactivity in the different types of instruments, the lower limit of $BDE[Ln^+\text{-OH}] \geq 499$ kJ/mol that would be established by reaction (3′) under truly thermal conditions is considered as only tentative for Ln = Eu, Tm and Yb until these reactions at low energies are confirmed or refuted.

Low-abundance products in addition to $LnOH^+$ in Figure 1 include $Eu(O_2)^+$ and TmO^+. In a SIFT study of the reaction $Ln^+ + O_2$ in ~1 Torr He, adducts $Ln(O_2)^+$ were similarly formed, presumably via an intermediate $[Ln(O_2)^+\bullet(He)]$.[46] In the QIT with a lower He pressure of $\sim10^{-4}$ Torr, O_2-addition was observed only for Eu^+, suggesting higher stability of adduct $Eu(O_2)^+$ compared with other $Ln(O_2)^+$. The oxide TmO^+ is presumably from reaction of Tm^+ with H_2O or O_2, both of which should be nearly thermoneutral processes given similarity between the *BDEs* for the bonds that are formed and broken: $BDE[Tm^+\text{-O}] = 485\pm13$ kJ/mol[55]; $BDE[H_2\text{-O}] = 491$ kJ/mol; $BDE[\text{O-O}] = 498$ kJ/mol.[30] In SIFT studies of reactions of Tm^+ with H_2O and O_2, formation of TmO^+ was not observed and it was noted there that the reactions were expected to be slightly endothermic—by less than ~20 kJ/mol—or very slightly exothermic.[29, 46] As with the hydroxide results above, the discrepancy between SIFT and QIT might reflect ion excitation in

the latter. For these oxidation reactions the thermodynamic constraint would require minor, if any, excitation to enable formation of TmO^+ from the reaction of Tm^+ with O_2 or H_2O.

FTICR-MS was employed by Marçalo and co-workers to study reactions of lanthanide ions Ln^+ with phenol, methanol, ethanol and isopropanol.[31, 32] Reaction (3) was observed with all four alcohols for Ln = Eu, with the phenol reaction establishing $BDE[Eu^+\text{-}OH] \geq BDE[C_6H_5\text{-}OH] = 474\pm8$ kJ/mol. This limit is close to that from reaction (3′) (499 kJ/mol), with both limits higher than previously reported $BDE[Eu^+\text{-}OH] = 423\pm7$ kJ/mol.[36] Because all of the alcohol BDE[R-OH] are below BDE[H-OH], reaction (3′), if it occurs under thermal conditions for Ln = Eu, Tm and Yb, would indicate that reaction (3) with alcohols should also be exothermic.

The result that Tm^+ and Yb^+ did not exhibit reaction (3) with any alcohol may suggest kinetic rather than thermodynamic barriers. Kinetic control of lanthanide cation reactivity, including with alcohols and water,[29, 32, 45] has been found to generally correlate with energies to excite the Ln^+ to an electronic configuration with two non-4f valence electrons outside of the xenon core, specifically a configuration $[Xe]4f^{n-2}5d^16s^1$. This relationship between reactivity and electronic configuration is attributed to inert character of the quasi-core 4f electrons, which results in a need for outer valence 5d and 6s electrons to achieve bond activation and insertion. The lanthanide cations studied here—Eu^+, Tm^+ and Yb^+—have relatively high excitation energies to $[Xe]4f^{n-2}5d^16s^1$ configurations and generally exhibit correspondingly lower reactivities compared with other Ln^+.[29, 32, 45] Notably, although Yb^+ is often found to be the least reactive lanthanide cation, the present QIT results indicate higher reactive for Yb^+ versus Tm^+.

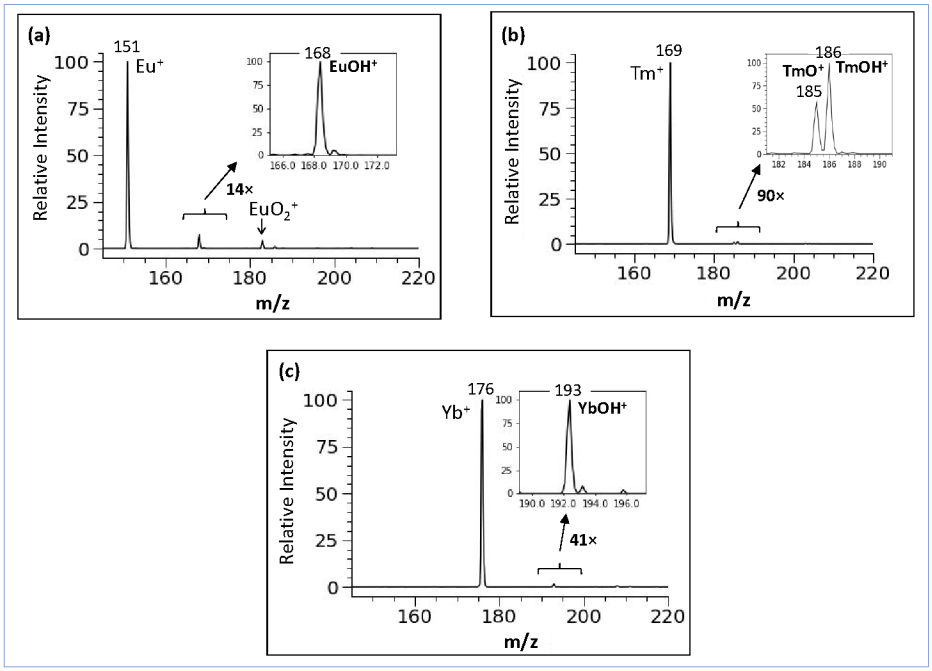

Figure 1. Mass spectra acquired after isolation of bare metals ions for 10 s in the ion trap, with the recorded ion intensity in arbitrary instrumental unites in parentheses: (a) Eu^+ (1.2×10^5); (b) Tm^+ (5.4×10^5); (c) Yb^+ (3.9×10^4). Background pressures may vary between experiments. Low product intensities after 10 s indicate inefficient reactions.

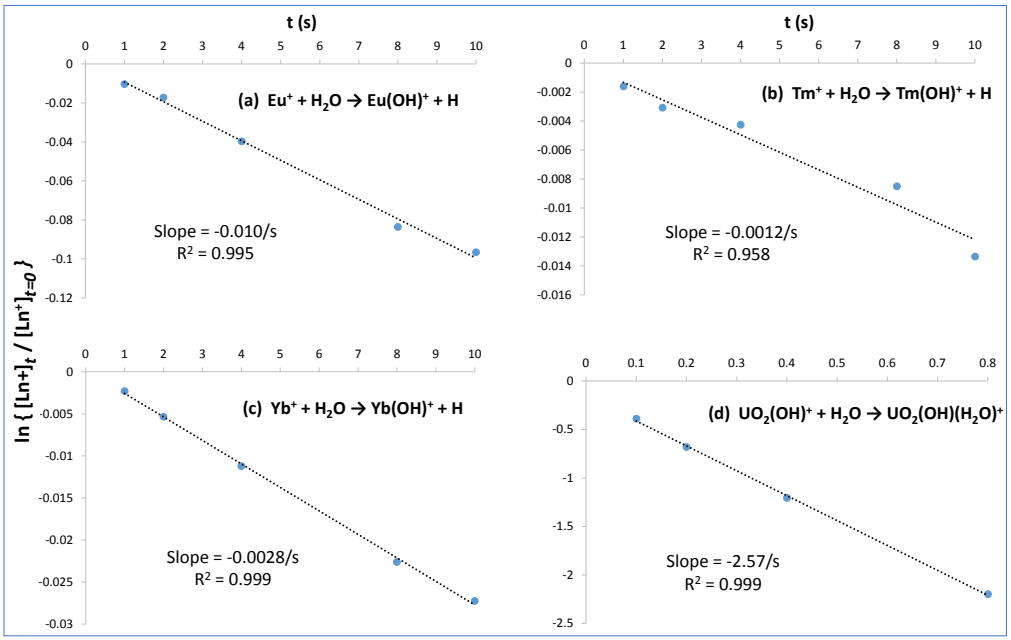

Figure 2. Pseudo-first order decay plots for the indicated reactions of water with (a) Eu^+; (b) Tm^+; (c) Yb^+; and (d) $UO_2(OH)^+$.

Table 1. Kinetics for reaction (3′).

Ln^+	Present QIT Results			k'/k_{col} from SIFT[29]	
	rate (s^{-1})[a]	Normalized[b]	Est. ~k'/k_{col}[c,d]	k'/k_{col}[c,e]	Normalized[b]
Eu^+	9.8×10^{-3}	400	~1.4×10^{-4}	≤ 2.4×10^{-4}	≤ 10
Tm^+	9.8×10^{-4}	40	~1.4×10^{-5}	≤ 2.4×10^{-4}	≤ 10
Yb^+	2.4×10^{-3}	100	~3.5×10^{-5}	2.5×10^{-3}	100

[a]Experimental reaction rate adjusted to a constant background water pressure.

[b]Relative rate normalized to 100 for Yb^+.

[c]Pseudo-first order rate constant k′ relative to collisional constant $k_{col} = 2.1\times10^{-9}$ cm^3 $molecule^{-1}$ s^{-1} (= 6.8×10^7 $Torr^{-1}$ s^{-1}).[29]

[d]Using approximate k′ obtained by assuming $P[H_2O] \approx 10^{-6}$ Torr.

[e]Reported products: $Yb(OH)^+$ from reaction (3′); hydrates $Eu(H_2O)^+$ and $Tm(H_2O)^+$.

(ii) Comparing hydroxides and halides

The result that reaction (3′) for Ln = Eu and Yb establishes minima for Ln^+-OH *BDEs* above the few uncertain literature values motivates further comparison with halides.[56] Figure 3 summarizes results of *BDE* assessments for lanthanide monohalides by Kaledin, Heaven and Field (*KHF*) in 1999,[57] and Chervonnyi and Chervonnaya (*C&C*) in 2007,[58] with little new information reported since then. *KHF* employed a ligand field approach to complement experimental *BDEs*, whereas *C&C* combined experimental data with estimates. Both assessments include predictions for experimentally unstudied Pm. For cases where *C&C* provided two *BDEs* for a LnF^+, both are in Figure 3, with designation of a value as *preferred*, rather than *alternate*, based primarily on minimizing variations in the difference *BDE*[Ln^+-F] -

BDE[Ln^+-Cl] (see below and Figure S6). Also identified in Figure 3 are the lower limits, *BDE*[Ln^+-F] ≥ *BDE*[C_6H_5-F] = 534±9 kJ/mol and *BDE*[Ln^+-Cl] ≥ *BDE*[C_6H_5-Cl] = 406±8 kJ/mol,[30] established for all Ln (except Pm) by reactions (4) and (5) (Table S2).[59]

(4) $Ln^+ + C_6H_5F \rightarrow LnF^+ + C_6H_5$ $\Delta E_4 = BDE[C_6H_5\text{-F}] - BDE[M^+\text{-F}]$

(5) $Ln^+ + C_6H_5Cl \rightarrow LnCl^+ + C_6H_5$ $\Delta E_5 = BDE[C_6H_5\text{-Cl}] - BDE[M^+\text{-Cl}]$

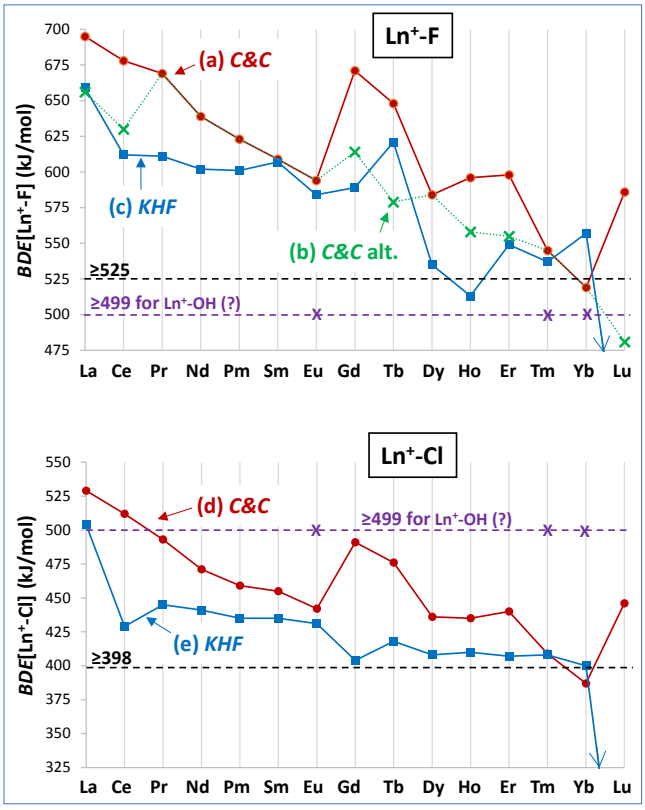

Figure 3. *BDEs* from *C&C*[58] and *KHF*.[57] (a) Ln^+-F *preferred* from *C&C* (red circles); (b) Ln^+-F *alternate* from *C&C* (green crosses); (c) Ln^+-F from *KHF* (blue squares); (d) Ln^+-Cl from *C&C* (red circles); and (e) Ln^+-Cl from *KHF* (blue squares). Values off-scale: (c) *BDE*[Lu^+-F] = 377 kJ/mol; (e) *BDE*[Lu^+-Cl] = 181 kJ/mol. Dashed lines are lower limits: *tentative* limit of 499 kJ/mol for $LnOH^+$ from reaction (3′) (Ln = Eu, Tm and Yb from this work); 525 kJ/mol for LnF^+ from reaction (4); 398 kJ/mol for $LnCl^+$ from reaction (5).[59]

Although *BDEs* from *KHF* and *C&C* in Figure 3 exhibit some similar trends, disparities include the much higher *BDE*[Gd^+-X] and *BDE*[Lu^+-X] from *C&C*. The *KHF* values for *BDE*[Lu^+-F] (377 kJ/mol) and *BDE*[Lu^+-Cl] (181 kJ/mol) are evidently too low, with the latter well below the experimental value of 473±68 kJ/mol.[60] The *C&C* values for LuF^+ and $LuCl^+$ seem more reasonable, though uncertain. The *preferred C&C* values in Figure 3 correspond to an increase of 77 kJ/mol from *BDE*[Eu^+-F] (594 kJ/mol) to *BDE*[Gd^+-F] (671 kJ/mol), which is in accord with the difference of 87 kJ/mol from high-temperature equilibria (*BDE*[Eu^+-F] = 482 kJ/mol; *BDE*[Gd^+-F] = 569 kJ/mol[61, 62]). Another evaluation of the assessed *BDEs* is the difference *BDE*[Ln^+-F] - *BDE*[Ln^+-Cl] ($\Delta BDE[Ln^+F/Cl]$). As the nature of fluoride and chloride bonding is presumed similar, $\Delta BDE[Ln^+F/Cl]$ is expected to change gradually and regularly

across the lanthanide series. This difference ranges from 132 kJ/mol to 180 kJ/mol for the *preferred C&C BDEs*,[58] but more irregularly and over a larger range of 103 kJ/mol to 203 kJ/mol for the *KHF BDEs* (Table S4 and Figure S6).[57] This comparison partly reflects that the *preferred C&C* values were identified specifically as those that exhibit smaller variations in Δ*BDE*[Ln^+F/Cl]. Although not all of the *preferred C&C BDEs* are necessarily the most accurate, they are considered overall most reliable.

The *preferred C&C BDE*[Ln^+-F] in Figure 3 are in accord with the lower limit from reactions (4) and (5), except for *BDE*[Yb^+-F] (519 kJ/mol), which is slightly below the limit of 525 kJ/mol. For neutral YbF there is a previous estimate of *BDE*[Yb-F] ≈ 467 kJ/mol from spectroscopic results,[63] and a lower limit of *BDE*[Yb-F] ≥ 518±10 kJ/mol from chemiluminescence spectra.[64] The resulting values for cationic YbF^+ derived from equation (2) using IE[YbF] = 570±5 kJ/mol[35] and IE[Yb] = 602.6 kJ/mol[30] are *BDE*[Yb^+-F] ≈ 500 kJ/mol and *BDE*[Yb^+-F] ≥ 551 kJ/mol. Although *BDE*[Yb^+-F] = 519 kJ/mol from *C&C* may be slightly too low, the actual value is basically unknown.

In analogy with the above comparison of fluorides and chlorides, the fluoride/hydroxide difference, *BDE*[Ln-F] - *BDE*[Ln-OH] (Δ*BDE*[LnF/OH]), should also be comparable for different Ln.[28, 65] For other similar metals, Brutti et al. estimated this fluoride/hydroxide difference as ~140 kJ/mol,[34] with the values for barium illustrative: *BDE*[Ba-F] = 581 kJ/mol;[30] *BDE*[Ba-Cl] = 432 kJ/mol;[66] *BDE*[Ba-OH] = 444 kJ/mol.[30] As the case of barium exemplifies, chloride and hydroxide *BDEs* are often similar to one another, with both roughly 140 kJ/mol below those for fluorides. Using the *preferred C&C BDE*[Ln^+-F] values and the tentative limit of *BDE*[Ln^+-OH] ≥ 499 kJ/mol from reaction (3′), the following tentative upper limits for Δ*BDE*[Ln^+F/OH] are obtained: ≤95 kJ/mol for Eu, ≤46 kJ/mol for Tm, and ≤20 kJ/mol for Yb. All three limits are below the typical difference of ~140 kJ/mol, which if valid could suggest unusually similar bonding in these lanthanide fluorides and hydroxides. However, it should be re-emphasized that because the reactivity identified here for these three Ln^+ is at odds with previous results using other well-established techniques,[29, 45] these new limits are provisional. Additionally, the other relevant *BDEs* needed for comparison, such as that for YbF^+, are too uncertain (or unknown) to allow for definitive conclusions.

(iii) Comparing neutrals and cations (peculiar Lu)

If ionization energies are known, equation (2) allows conversion of *BDEs* for neutral fluorides LnF to those for cations LnF^+, to allow comparison with hydroxides $LnOH^+$ as are characterized by reaction (3′). Additionally, equation (2) is a fundamental relationship between *BDEs* of neutrals and cations, expressing that if IE[Ln] is above IE[LnX], then *BDE*[Ln^+-X] is above *BDE*[Ln-X]. Plotted in Figure 4 are values for *BDE*[Ln^+-F] - *BDE*[Ln-F] (Δ*BDE*[LnF^+/LnF]) using *BDEs* from both the *preferred C&C*[58] and *KHF* values.[57] The Δ*BDE*[LnF^+/LnF] from *C&C* are positive and generally decrease from La to Yb, then sharply decreasing to a negative value for Lu. This "Lu anomaly" is reminiscent of other characteristics possibly suggesting Lu is not a proper lanthanide.[67] Another striking aspect of the lutetium

values in Figure 4 is the large disparity between Δ*BDE*[LuF^+/LuF] from *C&C* versus *KHF*. Because IE[Ln] are accurately known (e.g., IE[Lu] = 523.5168±0.0012 kJ/mol[68]), discrepancies in Δ*BDE*[LnF^+/LnF] reflect uncertainties in IE[LnF], such as for LuF. Estimates for IE[LuF] include a wide range of 630±100 kJ/mol based on general trends,[61] and 666 kJ/mol from an ionic bonding model.[23] The *preferred* *BDE*[Lu^+-F] from *C&C* instead employs an estimate of IE[LuF] ≈ 585 kJ/mol, which provides the relatively high *BDE*[LuF^+] in Figure 3 and the less negative Δ*BDE*[LuF^+/LuF] in Figure 4.

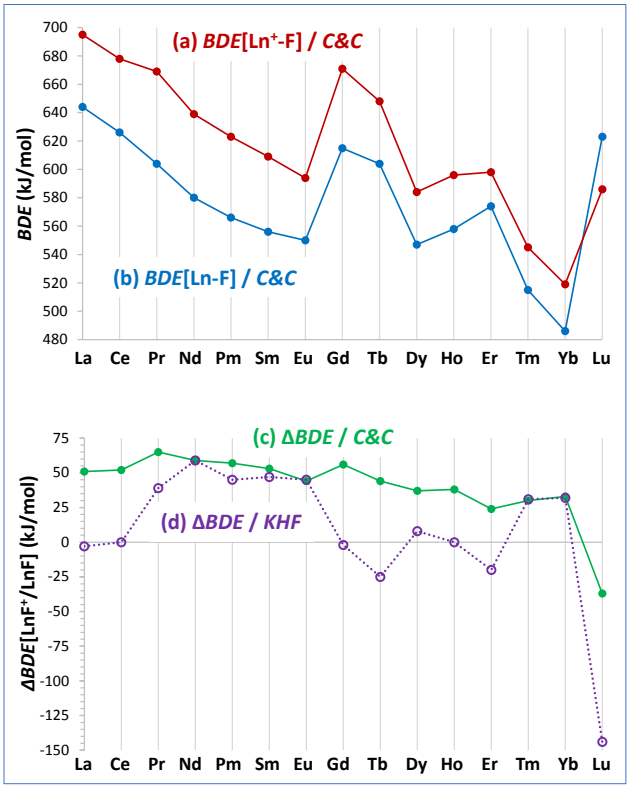

Figure 4. *BDEs* for (a) cation LnF^+ from *C&C* (*preferred* in Fig. 3a); and (b) neutral LnF from *C&C*[58]. Difference Δ*BDE*[LnF^+/LnF] = IE[Ln] – IE[LnF]: (c) from *C&C*; and (d) from *KHF*.[57]

As LuF illustrates, even such an elementary parameter as IE[LuX] is often too uncertain to fully assess effects of ionization on bonding in LnX. Nonetheless, results in Figure 4 reveal a clear change in this effect between Δ*BDE*[YbF^+/YbF] and Δ*BDE*[LuF^+/LuF], with the value for the latter distinctively negative. This characteristic of lutetium can be attributed to a relatively low IE[Lu], 80.4 kJ/mol lower than IE[Yb],[68] and a relatively high albeit uncertain IE[LuF]. For some diatomics, like H_2 and Be_2, there are large changes in the *BDE* upon ionization due to obvious changes in bonding. Disruption of the covalent H:H bond by removal of a bonding electron results in a decrease from *BDE*[H_2] = 436 kJ/mol to *BDE*[H_2^+] = 260 kJ/mol.[30] Neutral Be:···:Be is bound by a weak Van der Waals interaction, with ionization resulting in formation of a partial covalent bond and an increase from *BDE*[Be_2] = 13 kJ/mol to *BDE*[Be_2^+] = 197 kJ/mol.[69, 70]

The bond in $LnX^{0/+}$ is necessarily more polar than in homonuclear diatomics like H_2 and Be_2. The fully ionic extreme of a polarization is transfer of an electron from electropositive Ln to electronegative X, with the resulting Coulomb interaction comprising the bond. Fully ionic neutral LnX is represented as $(Ln^+)(X^-)$ and cation LnX^+ as $(Ln^{2+})(X^-)$, with thermodynamic pathways for ionic bond dissociation energies, BDE_{ionic}, in Scheme 1 and equations (6a)-(6c). In these pathways, EA[X] is the electron affinity of X, and E_C is the Coulomb interaction energy between anion X^- ($q_1 = -1$) and cation Ln^+ or Ln^{2+} ($q_2 = +1$ or +2) separated by distance r ($E_C = -[1389.4\ (kJ/mol)(Å)/(e)^2][q_1q_2/r]$). Considering the example of LaF, the estimated distance r = 2.02 Å[71] gives E_C = -688 kJ/mol; inserting this energy in equation (6a) along with IE[La] = 538 kJ/mol[68] and EA[F] = -328 kJ/mol[30] yields BDE_{ionic}[La-F] = 478 kJ/mol. For cation LaF^+, (r = 1.97 Å; E_C = -1411 kJ/mol; IE[La^+] = 1079 kJ/mol), equation (6b) yields BDE_{ionic}[La^+-F] = 660 kJ/mol. The latter is remarkably—likely fortuitously—close to *BDE*[La^+-F] from *C&C* (695 kJ/mol and 656 kJ/mol).[58] As $LnX^{0/+}$ bond distances decrease from La to Lu due to the lanthanide contraction, Coulomb energies become more negative and their contributions to BDE_{ionic} more positive. However, the change in E_C across the entire lanthanide series is only ~36 kJ/mol for LnF, and ~76 kJ/mol for LnF^+, which is less than 6 kJ/mol between adjacent lanthanides (see Figure S7).

(6a) $BDE_{ionic}[Ln\text{-}X] = -IE[Ln] - EA[X] - E_C[(Ln^+)(X^-)]$

(6b) $BDE_{ionic}[Ln^+\text{-}X] = -IE[Ln^+] - EA[X] - E_C[(Ln^{2+})(X^-)]$

(6c) $\Delta BDE_{ionic}[LnX^+/LnX] = IE[Ln] - IE[Ln^+] + E_C[(Ln^+)(X^-)] - E_C[(Ln^{2+})(X^-)]$

Whereas differences in Coulomb energy E_C across the lanthanide series are small and regular, larger differences are found for IE[Ln], IE[Ln^+] and IE[Ln]-IE[Ln^+], and thus also for BDE_{ionic}[Ln-F], BDE_{ionic}[Ln^+-F] and ΔBDE_{ionic}[LnX^+/LnX] (Figure 5). For Lu, a relatively low IE[Lu] and high IE[Lu^+] are manifested as a high BDE_{ionic}[Ln-F], low BDE_{ionic}[Ln^+-F] and negative ΔBDE_{ionic}[LuF^+/LuF]. The ionic model thus predicts the distinctive decrease in the *BDE* of LuF upon ionization, and the increase in *BDEs* from neutrals YbF to LuF. However, it also predicts a decrease in *BDEs* from cations YbF^+ to LuF^+, which is not observed using the *preferred C&C* values, though it is apparent for the *alternate C&C* and *KHF* values (Figure 3). The ionic model also fails to predict the maxima in *BDEs* at $GdF^{0/+}$. Although the ionic model may have relevance to the nature of $LnF^{0/+}$ molecules, it does not account for key variations in *BDEs*.

The ionic model can also be used to predict variations in BDE_{ionic} upon changing the halide/hydroxide constituent X. The difference between equation (6a) for X = F and X = OH yields equation (6d), where $\Delta BDE_{ionic}[LnF/OH] = BDE_{ionic}[Ln\text{-}F] - BDE_{ionic}[Ln\text{-}OH]$. As the ionic radius of OH^- is only ~3% larger than that of F^-,[72] E_C for X =F is less than 20 kJ/mol more negative than for X = OH. The much larger difference between EA[F] (-328 kJ/mol) and EA[OH] (-174 kJ/mol)[30] thus dominates ΔBDE_{ionic}[LnF/OH], which estimated as ~170 kJ/mol is roughly comparable to ΔBDE[BaF/OH] (137 kJ/mol).[34] In view of uncertainties described above, it remains to be determined if ΔBDE_{ionic}[LnF/OH] predicted by the ionic model is consistently, occasionally, or never manifested in ΔBDE[LnF/OH].

$$(6d) \quad \Delta BDE_{\text{ionic}}[\text{LnF/OH}] = E_C[(Ln^+)(OH^-)] - E_C[(Ln^+)(F^-)] + EA[OH] - EA[F]$$

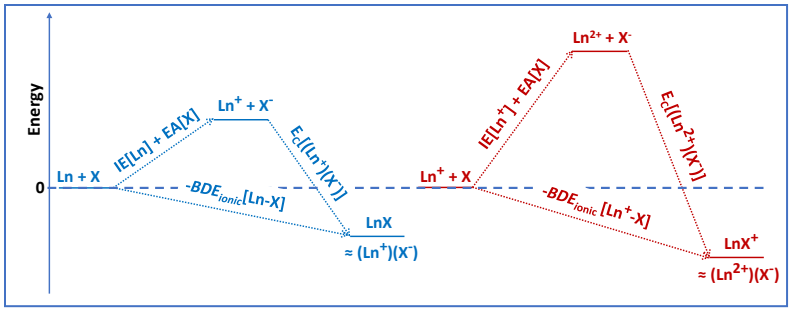

Scheme 1. Thermodynamic pathways to obtain the fully ionic *BDE* (BDE_{ionic}) for LnX (left) and LnX^+ (right). Parameters are ionization energy (IE), electron affinity (EA), and Coulomb interaction energy (E_C).

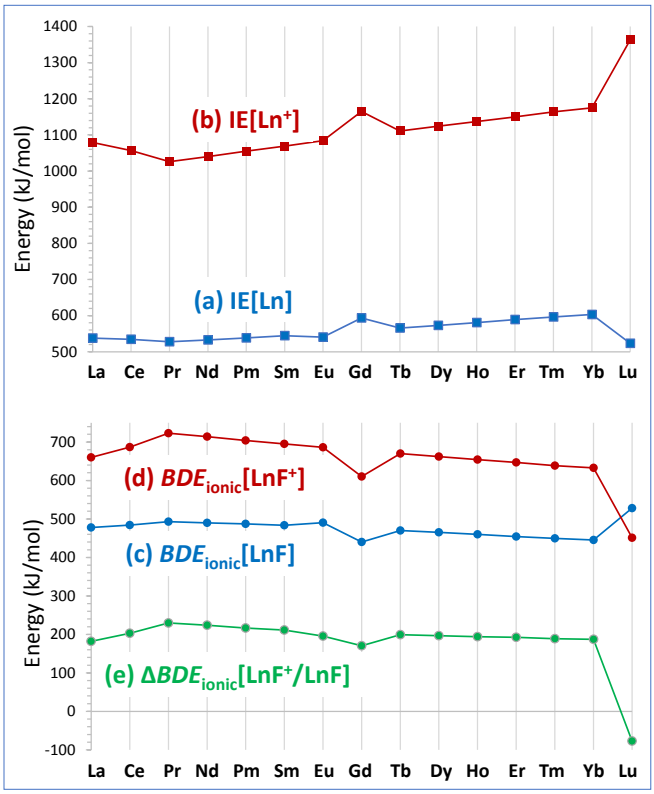

Figure 5. Ionization energies of (a) Ln (top/blue squares) and (b) Ln^+ (top/red squares).[68] Estimated purely ionic *BDEs* for (c) LnF (bottom/blue circles), (d) LnF^+ (bottom/red circles) and difference (d)-(c) (bottom/green circles).

(iv) Computational results for BDEs for hydroxides and fluorides

Dixon and co-workers reported computed energies for reactions that produce LnF and LnOH.[28, 65] Although *BDEs* were not the primary goal of that work, they follow from the reported energies. As all of the computations—from 2011 for fluorides[65] and 2017 for hydroxides[28]—employed a coupled cluster CCSD(T) level of theory using the same basis sets, it is reasonable to compare the results. Computed *BDE*[LnF] plotted in Figure 6 (values in Table S3) are from the U/UCCSD(T)/aug-cc-pVDZ+Stuttgart(Ln) energies for the reaction Ln + CH_3F → LnF + CH_3 (Table 6 in ref.[65]), and using $BDE[CH_3\text{-}F]$ = 459.4 kJ/mol.[30] The *BDE*[LnOH] are from the R/UCCSD(T)/aug-cc-pVDZ+Stuttgart(Ln) energies for the reaction Ln + H_2O_2 →

LnOH + OH (Table 7 in ref.[28]), and using *BDE*[HO-OH] = 214.1 kJ/mol.[30] The authors of the computational work provided details about their rationale for selection of the particular methods and basis sets.[28, 65] For the first half of the series, La to Gd, the computed *BDE*[Ln-F] are in good accord with the *C&C* values in Figure 6 (top), with a maximum deviation of 39 kJ/mol for CeF. In the second half, the computed *BDE*[Ln-F] are in satisfactory agreement with reported values for Ln = Dy, Er, Tm and Yb, but for Ln = Tb, Ho and Lu they are higher by 117-190 kJ/mol, which is beyond the uncertainty range of the *C&C* values.

Trends in Figure 6 for the computed *BDE*[Ln-OH] generally parallel those for *BDE*[Ln-F], as highlighted by the plotted *BDE*[Ln-F] - *BDE*[Ln-OH] (Δ*BDE*[LnF/OH]). For most Ln, Δ*BDE*[LnF/OH] is in the range 100-140 kJ/mol, which is similar to other metals,[34] but for Gd and Er it is anomalously small and for Dy it is uniquely negative. As for cationic LnF^+ and $LnOH^+$ discussed above, the assumption that Δ*BDE*[LnF/OH] for neutrals is constant, or even necessarily positive, has not been fully established. The variations in computed Δ*BDE*[LnF/OH] are intriguing, particularly given the unexpectedly small Δ*BDE*[Yb^+F/OH] tentatively suggested by the present results. Notably, the three lanthanides for which the computed Δ*BDE*[LnF/OH] are distinctive—Gd, Dy and Er—are different from those—Tb, Ho and Lu—for which the computed *BDE*[Ln-F] are too high. All six of these anomalies are in the second half of the lanthanide series, where electron correlation of multiple 4f electrons, and obtaining the correct spin localization and coupling, introduces particular computational challenges.[73, 74] Computational limitations such as revealed in Figure 6 are to be expected given benefits of multiconfigurational treatment for such molecules.[71, 73] For the lanthanides emphasized here—Eu, Tm and Yb—the computed *BDE*[LnF] and *BDE*[LnOH] agree with experiment to within 27 kJ/mol, and the computed Δ*BDE*[LnF/OH] are in an expected range of 124-134 kJ/mol, rather than <100 kJ/mol as suggested in the above discussion. However, the computations considered neutrals rather than cations as were experimentally studied in the present work.

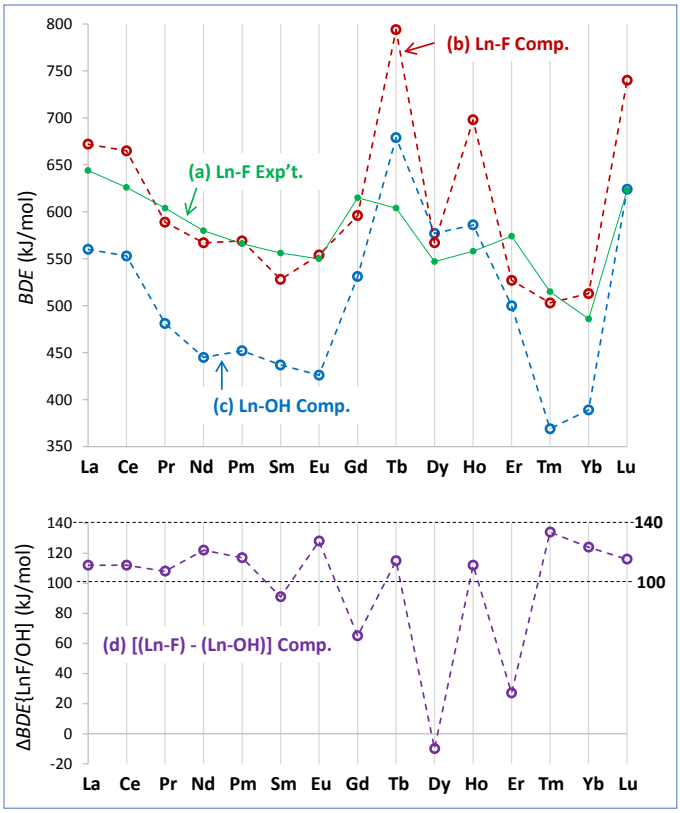

Figure 6. Computed and assessed experimental *BDEs*: (a) Ln-F experimental/estimated from *C&C*;[58] (b) Ln-F from CCSD(T) computations;[65] (c) Ln-OH from CCSD(T) computations;[28] (d) Difference between computed Ln-F and Ln-OH ((b)-(c)). Dashed lines at 100 and 140 kJ/mol in the bottom plot identify an expected range based on other metals.

(v) Possibilities for advancing understanding

Further experiments and computations are clearly needed to resolve large uncertainties in lanthanide halide and hydroxide *BDEs*. A specific need is comparisons between fluorides and hydroxides, such as between possibly similar *BDE*[Yb^+-F] and *BDE*[Yb^+-OH] highlighted here. Experimental *BDEs* for small metal-containing molecules, including neutral and cationic $LnX^{0/+}$, are mostly from high-temperature equilibria.[75] Measured or estimated ionization energies in conjunction with equation (2) provide *BDEs* for cations from neutrals.[58] Although traditional experimental approaches have provided seminal information, the extreme conditions of high-temperature and reactive gases impose formidable challenges. Furthermore, large uncertainties in most IE[LnX] preclude using equation (2) to obtain reliable differences between neutrals and cations, as revealed by large disparities between the three sets of *BDE*[Ln^+-F] in Figure 3.

An alternative experimental approach for *BDEs* of small metal-containing molecules is guided ion beam mass spectrometry (GIBMS) as advanced by Armentrout.[76] In GIBMS, the kinetic energy dependence of an ion-molecule reaction provides the *BDE*. The approach has been applied to many small cationic molecules including ThO^+,[77] ThN^+, [78] and CeH^+,[79] and $PtCl^+$.[80] GIBMS would be applicable to LnF^+ and $LnOH^+$ produced by endothermic reactions. A potential reaction to yield LnF^+ is $Ln^+ + BF_3$. The bonds in BF_3 are sufficiently strong—*BDE*[F_2B-F] =

625 kJ/mol[30]—that the reaction with most Ln^+ to yield LnF^+ should be endothermic, almost certainly so for the key species YbF^+. As discussed above, it remains uncertain whether the reaction of Yb^+ with H_2O to yield $YbOH^+$ is endothermic as expected from previous results, or exothermic as tentatively suggested by the present QIT results, a dichotomy that could be resolved by GIBMS. If reaction (3′) to yield $YbOH^+$ is indeed endothermic, then its GIBMS threshold energy should provide a refined value for *BDE*[Yb^+-OH].

Another route to accurate *BDEs* of metal-containing diatomics is predissociation threshold (PDT) spectroscopy as demonstrated by Morse et al.[81] A basic requirement of PDT is that the *BDE* of the neutral is lower than its IE. This condition is presumably not met by particularly strongly bound lanthanide fluorides like NdF and TbF, but others like YbF should meet it.[57] Another PDT constraint is the necessity for a high density of electronic states near the *BDE*, which is likely the case for most LnX, but perhaps not so for those with a filled $4f^{14}$ sub-shell,[82] which may preclude effective application of PDT to YbF and YbOH.[68]

The computed *BDE*[Ln-F] considered here exhibit good agreement with reported values for all LnF, except TbF, HoF and LuF. Although such specific discrepancies could likely be resolved by computational refinements, it is desirable to identify and address underlying problems to advance towards truly predictive theory. Computations of Δ*BDE*[LnF/OH] would illuminate the large divergences in this parameter tentatively predicted for Ln = Gd, Dy and Er, and for Δ*BDE*[Ln^+F/OH] they would elucidate the issue of possibly similar *BDEs* for YbF^+ and $YbOH^+$. Computed Δ*BDE*[LnF/OH] were here obtained by combining reactions (7a) and (7b) (X = F; Y = OH) to yield (7c). Sources of error for (7a) and (7b) include disparate and complex electronic configurations of the Ln as an atom versus bound in LnX. Such errors should largely cancel upon summing reactions (7a) and (7b), but a more direct evasive approach is to compute exchange reaction (7c). For X = F and Y = OH, this would address the fluctuations apparent in Figure 6d. Reaction (7c) for "hard" fluoride, X = F, and "softer" halide, Y = Cl, Br or I, could reveal trends due to variations in bond covalency for different halides and lanthanides.

(7a) $LnX \rightarrow Ln + X$ $\quad \Delta E_{7a} = BDE[Ln\text{-}X]$

(7b) $Ln + Y \rightarrow LnY$ $\quad \Delta E_{7b} = -BDE[Ln\text{-}Y]$

(7c) $LnX + Y \rightarrow LnY + X$ $\quad \Delta E_{7c} = BDE[Ln\text{-}X] - BDE[Ln\text{-}Y]$

Conclusions

A possible product of the bimolecular reaction of lanthanide ion Ln^+ and H_2O is hydroxide $LnOH^+$. Under low-energy conditions this reaction establishes a bond dissociation energy limit, *BDE*[Ln^+-OH] ≥ *BDE*[H-OH] (499 kJ/mol). This reaction was previously reported in one study to occur for Ln = Yb, but not for Eu or Tm,[29] while in another study it was not observed for all three of these Ln.[45] In contrast, it was here found that all three of these Ln exhibit this reaction, albeit very inefficiently, in a quadrupole ion trap. If the reactions in the ion trap occur under thermal or near-thermal conditions, the resulting minimum of 499 kJ/mol for the three *BDE*[Ln^+-OH] would be in discord with previously reported but quite uncertain values

for Ln = Eu and Yb. However, the new *BDE* minimum is considered tentative until confirmation that the reactions occur under truly thermal conditions.

Given that hydroxides are often assessed as pseudo-halides, the unexpected new results for hydroxides motivated closer consideration of isoelectronic fluorides. Despite uncertainties in *BDE*[Ln^+-F], comparison of available values with the new minima for *BDE*[Ln^+-OH] suggests unexpectedly strong hydroxide bonding that is similar to fluorides. In particular, if the new tentative limits for *BDE*[Ln^+-OH] are valid, this quantity would be within less than ~100 kJ/mol of *BDE*[Ln^+-F] for Ln = Eu and Tm, and within less than ~50 kJ/mol for Ln = Yb. These possible differences are significantly smaller than for other metals like barium, for which the *BDE* of BaOH is ~140 kJ/mol lower than that of BaF. Although the lanthanide results tentatively suggest unusually comparable bonding in hydroxides and fluorides, most available *BDEs* for these species are insufficiently accurate for definitive comparisons and conclusions. Approaches like guided ion beam mass spectrometry,[76] and predissociation spectroscopy[81] could provide more reliable and extensive *BDEs* for key species like YbF, YbOH and LuF. Relating *BDEs* for neutral LnX and cation LnX^+ often relies on ionization energies of LnX, which are typically lacking but could be accurately determined using photoelectron spectroscopy approaches like PFI-ZEKE.[83] A particularly desirable target is IE[LuF] to refine the evidently distinctive relationship whereby *BDE*[Lu^+-F] is significantly lower than *BDE*[Lu-F]. Ab initio computations of *BDEs* for neutral and cationic $LnF^{0/+}$ and $LnOH^{0/+}$ are challenging due to uncertainties for the separated fragments, particularly for lanthanide atoms with partly filled 4f sub-shells. Some of the computational complications could be circumvented using *BDE* differences from ligand-exchange reactions like $LnF^{0/+} + OH \leftrightarrow LnOH^{0/+} + F$.

Dissociation of LnX^+ formally corresponds to reduction from oxidation state $Ln^{(II)}$ to $Ln^{(I)}$, with *BDEs* reflecting the relative stabilities of these states. *BDEs* for $Ln^{(II)}F^+$ (to $Ln^{(I)+} + F$) exhibit a maximum for Ln = La and minimum for Ln = Yb. The implication that $La^{(II)}$ is more stable than $Yb^{(II)}$ seems contrary to conventional behavior. However, decomposition of divalent lanthanide $Ln^{(II)}$ species in condensed phases is typically by oxidation to trivalent $Ln^{(III)}$ rather than reduction to monovalent $Ln^{(I)}$.[84-86] Whereas the lower stability of $La^{(II)}$ versus $Yb^{(II)}$ is relative to $La^{(III)}$ and $Yb^{(III)}$ under typical practical circumstances, dissociation of molecules like LnX^+ characterizes oxidation states from the very different perspective of $Ln^{(II)}$ relative to $Ln^{(I)}$.

Supporting Information

Summary of reported reactions of lanthanides with hydroxide and halide donors. Assessed and computed *BDEs* for lanthanide halides. ESI mass spectra of $LnCl_3$ solutions. Kinetics plots for reaction (3′) with background water, with added water, and for different ion isolation widths. Mass spectrum showing hydration of $UO_2(OH)^+$. Plot of difference between fluoride and chloride *BDEs*. Procedure and results for ionic *BDEs*.

Acknowledgement

This work was supported by the U.S. Department of Energy, Office of Science, Office of Basic Energy Sciences, Chemical Sciences, Geosciences, and Biosciences Division, Heavy Element Chemistry Program, at Lawrence Berkeley National Laboratory under Contract DE-AC02-05CH11231. The authors are grateful to an anonymous reviewer for pointing out reference 45.

References

1. Flynn, C. M., Hydrolysis of Inorganic Iron(III) Salts. *Chem Rev* **1984,** *84* (1), 31-41.
2. Cheng, F. Y.; Liang, J.; Tao, Z. L.; Chen, J., Functional Materials for Rechargeable Batteries. *Adv Mater* **2011,** *23* (15), 1695-1715.
3. Macdonald, D. D., Passivity - The Key to Our Metals-Based Civilization. *Pure Appl Chem* **1999,** *71* (6), 951-978.
4. Kastl, C.; Chen, C. T.; Kuykendall, T.; Shevitski, B.; Darlington, T. P.; Borys, N. J.; Krayev, A.; Schuck, P. J.; Aloni, S.; Schwartzberg, A. M., The Important Role of Water in Growth of Monolayer Transition Metal Dichalcogenides. *2D Mater* **2017,** *4* (2), 021024.
5. Myers, D. L.; Jacobson, N. S.; Bauschlicher, C. W.; Opila, E. J., Thermochemistry of Volatile Metal Hydroxides and Oxyhydroxides at Elevated Temperatures. *J Mater Res* **2019,** *34* (3), 394-407.
6. Schröder, D., Gaseous Rust: Thermochemistry of Neutral and Ionic Iron Oxides and Hydroxides in the Gas Phase. *J Phys Chem A* **2008,** *112* (50), 13215-13224.
7. Moeller, T.; Kremers, H. E., The Basicity Characteristics of Scandium, Yttrium, and the Rare Earth Elements. *Chem Rev* **1945,** *37* (1), 97-159.
8. Knope, K. E.; Soderholm, L., Solution and Solid-State Structural Chemistry of Actinide Hydrates and their Hydrolysis and Condensation Products. *Chem Rev* **2013,** *113* (2), 944-994.
9. Bünzli, J. C. G.; Andre, N.; Elhabiri, M.; Muller, G.; Piguet, C., Trivalent Lanthanide Ions: Versatile Coordination Centers with Unique Spectroscopic and Magnetic Properties. *J Alloy Compd* **2000,** *303*, 66-74.
10. Gandara, F.; Perles, J.; Snejko, N.; Iglesias, M.; Gomez-Lor, B.; Gutierrez-Puebla, E.; Monge, M. A., Layered Rare-Earth Hydroxides: A Class of Pillared Crystalline Compounds for Intercalation Chemistry. *Angew Chem Int Edit* **2006,** *45* (47), 7998-8001.
11. Geng, F. X.; Matsushita, Y.; Mat, R. Z.; Xin, H.; Tanaka, M.; Izumi, F.; Iyi, N.; Sasaki, T., General Synthesis and Structural Evolution of a Layered Family of $Ln_8(OH)_{20}Cl_4 \bullet nH_2O$ (Ln = Nd, Sm, Eu, Gd, Tb, Dy, Ho, Er, Tm, and Y). *J Am Chem Soc* **2008,** *130* (48), 16344-16350.
12. Lv, L.; Yang, Z. X.; Chen, K.; Wang, C. D.; Xiong, Y. J., 2D Layered Double Hydroxides for Oxygen Evolution Reaction: From Fundamental Design to Application. *Adv Energy Mater* **2019,** *9* (17), 1803358.
13. Yoshinari, N.; Meundaeng, N.; Tabe, H.; Yamada, Y.; Yamashita, S.; Nakazawa, Y.; Konno, T., Single-Crystal-to-Single-Crystal Installation of $Ln_4(OH)_4$ Cubanes in an Anionic Metallosupramolecular Framework. *Angew Chem Int Edit* **2020,** *59*, 18048-18053.
14. Vasiliu, M.; Hill, J. G.; Peterson, K. A.; Dixon, D. A., Structures and Heats of Formation of Simple Alkaline Earth Metal Compounds II: Fluorides, Chlorides, Oxides, and Hydroxides for Ba, Sr, and Ra. *J Phys Chem A* **2018,** *122* (1), 316-327.
15. Meschter, P. J.; Opila, E. J.; Jacobson, N. S., Water Vapor-Mediated Volatilization of High-Temperature Materials. *Annu Rev Mater Res* **2013,** *43*, 559-588.
16. Bogatko, S.; Cauet, E.; Geerlings, P., Influence of F- Coordination on Al^{3+} Hydrolysis Reactions from Density Functional Theory Calculations. *J Phys Chem C* **2011,** *115* (14), 6910-6921.
17. Mestdagh, J. M.; Visticot, J. P., Semiempirical Electrostatic Polarization Model of the Ionic Bonding in Alkali and Alkaline-Earth Hydroxides and Halides. *Chem Phys* **1991,** *155* (1), 79-89.
18. Hudson, E. R., Laser Cooling of Larger Quantum Objects. *Science* **2020,** *369* (6509), 1304-1305.

19. Denis, M.; Haase, P. A. B.; Timmermans, R. G. E.; Eliav, E.; Hutzler, N. R.; Borschevsky, A., Enhancement Factor for the Electric Dipole Moment of the Electron in the BaOH and YbOH Molecules. *Phys Rev A* **2019,** *99* (4), 042512.
20. Prasannaa, V. S.; Shitara, N.; Sakurai, A.; Abe, M.; Das, B. P., Enhanced Sensitivity of the Electron Electric Dipole Moment from YbOH: The Role of Theory. *Phys Rev A* **2019,** *99* (6), 062502.
21. Kafader, J. O.; Ray, M.; Jarrold, C. C., Low-Lying Electronic Structure of EuH, EuOH, and EuO Neutrals and Anions Determined by Anion Photoelectron Spectroscopy and DFT Calculations. *J Chem Phys* **2015,** *143* (3), 034305.
22. Kaledin, A. L.; Heaven, M. C.; Field, R. W.; Kaledin, L. A., The Electronic Structure of the Lanthanide Monohalides: A Ligand Field Approach. *J Mol Spectrosc* **1996,** *179* (2), 310-319.
23. Gotkis, I., Field-Stimulated Electron Promotion from Core 4f Orbital to Out-of-Core Sigma-6s Orbital Phenomenon in Simple Lanthanide Compounds. *J Phys Chem* **1991,** *95* (16), 6086-6095.
24. Myers, C. E., Case for Covalent Bonding in Lanthanide Trihalides. *Inorg Chem* **1975,** *14* (1), 199-201.
25. Ionova, G.; Madic, C.; Guillaumont, R., Covalency Effects in the Standard Enthalpies of Formation of Trivalent Lanthanide and Actinide Halides. *Radiochim Acta* **1997,** *78*, 83-90.
26. Neidig, M. L.; Clark, D. L.; Martin, R. L., Covalency in F-Element Complexes. *Coordin Chem Rev* **2013,** *257* (2), 394-406.
27. Wang, S. G.; Schwarz, W. H. E., Lanthanide Diatomics and Lanthanide Contractions. *J Phys Chem* **1995,** *99* (30), 11687-11695.
28. Wang, X. F.; Andrews, L.; Fang, Z. T.; Thanthiriwatte, K. S.; Chen, M. Y.; Dixon, D. A., Properties of Lanthanide Hydroxide Molecules Produced in Reactions of Lanthanide Atoms with H_2O_2 and $H_2 + O_2$ Mixtures: Roles of the +I, +II, +III, and +IV Oxidation States. *J Phys Chem A* **2017,** *121* (8), 1780-1797.
29. Cheng, P.; Koyanagi, G. K.; Bohme, D. K., Gas-Phase Reactions of Atomic Lanthanide Cations with D_2O: Room-Temperature Kinetics and Periodicity in Reactivity. *ChemPhysChem* **2006,** *7* (8), 1813-1819.
30. Linstrom, P. J., NIST Chemistry WebBook, NIST Standard Reference Database Number 69 (https://webbook.nist.gov/chemistry/). National Institute of Standards and Technology: Gaithersburg, MD, USA, 2020.
31. Carretas, J. M.; de Matos, A. P.; Marçalo, J.; Pissavini, M.; Decouzon, M.; Géribaldi, S., Gas-Phase Reactivity of Rare Earth Cations with Phenol: Competitive Activation of C-O, O-H, and C-H Bonds. *J Am Soc Mass Spectr* **1998,** *9* (10), 1035-1042.
32. Carretas, J. A.; Marçalo, J.; de Matos, A. P., Gas-Phase Reactions of Lanthanide Cations with Alcohols. *Int J Mass Spectrom* **2004,** *234* (1-3), 51-61.
33. Belyaev, V. N.; Lebedeva, N. L., The Dissociation Energy of the YbOH Molecule. *Zh Fiz Khim* **1998,** *72* (12), 2176-2181.
34. Brutti, S.; Terai, T.; Yamawaki, M.; Yasumoto, M.; Balducci, G.; Gigli, G.; Ciccioli, A., Mass Spectrometric Investigation of Gaseous YbH, YbO and YbOH Molecules. *Rapid Commun Mass Spectrom* **2005,** *19* (16), 2251-2258.
35. Belyaev, V. N.; Lebedeva, N. L.; Krasnov, K. S., Electronic Energies and Ionization Potentials of YbX (X=F,OH,Cl,Br and I) Molecules. *Zh Fiz Khim* **1996,** *70* (8), 1429-1434.
36. Belyaev, V. N.; Lebedeva, N. L., Spectrophotometric study of $Eu^+ + H_2O \leftrightarrow EuOH^+ + H$ Equilibrium in Flames with Europium Additions. *Russ J Phys Chem A* **2010,** *84* (11), 1841-1850.
37. Rios, D.; Rutkowski, P. X.; Shuh, D. K.; Bray, T. H.; Gibson, J. K.; Van Stipdonk, M. J., Electron Transfer Dissociation of Dipositive Uranyl and Plutonyl Coordination Complexes. *J Mass Spectrom* **2011,** *46* (12), 1247-1254.

38. Rios, D.; Michelini, M. C.; Lucena, A. F.; Marçalo, J.; Bray, T. H.; Gibson, J. K., Gas-Phase Uranyl, Neptunyl, and Plutonyl: Hydration and Oxidation Studied by Experiment and Theory. *Inorg Chem* **2012,** *51* (12), 6603-6614.
39. Rutkowski, P. X.; Michelini, M. C.; Bray, T. H.; Russo, N.; Marçalo, J.; Gibson, J. K., Hydration of Gas-Phase Ytterbium Ion Complexes Studied by Experiment and Theory. *Theor Chem Acc* **2011,** *129* (3-5), 575-592.
40. Gronert, S., Estimation of Effective Ion Temperatures in a Quadrupole Ion Trap. *J Am Soc Mass Spectrom* **1998,** *9* (8), 845-848.
41. Nourse, B. D.; Kenttamaa, H. I., Effective Ion Temperatures in a Quadrupole Ion Trap. *J Phys Chem* **1990,** *94* (15), 5809-5812.
42. Lovejoy, E. R.; Wilson, R. R., Kinetic Studies of Negative Ion Reactions in a Quadrupole Ion Trap: Absolute Rate Coefficients and Ion Energies. *J Phys Chem A* **1998,** *102* (13), 2309-2315.
43. Cornehl, H. H.; Heinemann, C.; Marcalo, J.; deMatos, A. P.; Schwarz, H., The ''Bare'' Uranyl(2+) Ion, UO_2^{2+}. *Angewandte Chemie-International Edition in English* **1996,** *35* (8), 891-894.
44. Gibson, J. K.; Haire, R. G.; Santos, M.; Marçalo, J.; de Matos, A. P., Oxidation Studies of Dipositive Actinide Ions, An^{2+} (An = Th, U, Np, Pu, Am) in the Gas Phase: Synthesis and Characterization of the Isolated Uranyl, Neptunyl, and Plutonyl Ions UO_2^{2+}(g), NpO_2^{2+}(g), and PuO_2^{2+}(g). *J Phys Chem A* **2005,** *109* (12), 2768-2781.
45. Cornehl, H. H. Gas-Phase Ion Chemistry of f-Elements. PhD Thesis, Chemistry Department, Technical University of Berlin, 1997.
46. Koyanagi, G. K.; Bohme, D. K., Oxidation Reactions of Lanthanide Cations with N_2O and O_2: Periodicities in Reactivity. *J Phys Chem A* **2001,** *105* (39), 8964-8968.
47. Koyanagi, G. K.; Baranov, V. I.; Tanner, S. D.; Bohme, D. K., An Inductively Coupled Plasma/Selected-Ion Flow Tube Mass Spectrometric Study of the Chemical Resolution of Isobaric Interferences. *J Anal Atom Spectrom* **2000,** *15* (9), 1207-1210.
48. Koyanagi, G. K.; Lavrov, V. V.; Baranov, V.; Bandura, D.; Tanner, S.; McLaren, J. W.; Bohme, D. K., A Novel Inductively Coupled Plasma/Selected-Ion Flow Tube Mass Spectrometer for the Study of Reactions of Atomic and Atomic Oxide Ions. *Int J Mass Spectrom* **2000,** *194* (1), L1-L5.
49. Freiser, B. S., Investigation of Reactions of Metal-Ions and Their Clusters in the Gas-Phase by Laser-Ionization Fourier-Transform Mass-Spectrometry. *Talanta* **1985,** *32* (8b), 697-708.
50. Marshall, A. G.; Hendrickson, C. L.; Jackson, G. S., Fourier Transform Ion Cyclotron Resonance Mass Spectrometry: A Primer. *Mass Spectrom Rev* **1998,** *17* (1), 1-35.
51. Waters, T.; O'Hair, R. A. J.; Wedd, A. G., Catalytic Gas Phase Oxidation of Methanol to Formaldehyde. *J Am Chem Soc* **2003,** *125* (11), 3384-3396.
52. O'Hair, R. A. J., The 3D Quadrupole Ion Trap Mass Spectrometer as a Complete Chemical Laboratory for Fundamental Gas-Phase Studies of Metal Mediated Chemistry. *Chem Commun* **2006,** (14), 1469-1481.
53. Lucena, A. F.; Lourenço, C.; Michelini, M. C.; Rutkowski, P. X.; Carretas, J. M.; Zorz, N.; Berthon, L.; Dias, A.; Oliveira, M. C.; Gibson, J. K.; Marçalo, J., Synthesis and Hydrolysis of Gas-Phase Lanthanide and Actinide Oxide Nitrate Complexes: a Correspondence to Trivalent Metal Ion Redox Potentials and Ionization Energies. *Phys Chem Chem Phys* **2015,** *17* (15), 9942-9950.
54. Cooks, R. G.; Kaiser, R. E., Quadrupole Ion Trap Mass-Spectrometry. *Accounts Chem Res* **1990,** *23* (7), 213-219.
55. Murad, E.; Hildenbrand, D. L., Dissociation-Energies of GdO, HoO, ErO, TmO, and LuO - Correlation of Results for the Lanthanide Monoxide Series. *J Chem Phys* **1980,** *73* (8), 4005-4011.
56. Magnusson, E.; Moriarty, N. W., Binding Patterns in Single-Ligand Complexes of NH_3, H_2O, OH^-, and F^- with First Series Transition Metals. *Inorg Chem* **1996,** *35* (19), 5711-5719.

57. Kaledin, L. A.; Heaven, M. C.; Field, R. W., Thermochemical Properties (D^o and IP) of the Lanthanide Monohalides. *J Mol Spectrosc* **1999,** *193* (2), 285-292.
58. Chervonnyi, A. D.; Chervonnaya, N. A., Thermodynamic Properties of Lanthanum and Lanthanide Halides: IV. Enthalpies of Atomization of LnCl, $LnCl^+$, LnF, LnF^+, and LnF_2. *Russ J Inorg Chem* **2007,** *52* (12), 1937-1952.
59. Zhou, S. D.; Schlangen, M.; Schwarz, H., Mechanistic Aspects of the Gas-Phase Reactions of Halobenzenes with Bare Lanthanide Cations: A Combined Experimental/Theoretical Investigation. *Chem-Eur J* **2015,** *21* (5), 2123-2131.
60. Saloni, J.; Roszak, S.; Hilpert, K.; Popovic, A.; Miller, M.; Leszczynski, J., Mass Spectrometric and Quantum Chemical Studies of the Thermodynamics and Bonding of Neutral and Ionized LnCl, $LnCl_2$, and $LnCl_3$ Species (Ln = Ce, Lu). *Inorg Chem* **2006,** *45* (11), 4508-4517.
61. Zmbov, K. F.; Margrave, J. L., Mass Spectrometric Studies of Scandium Yttrium Lanthanum and Rare-Earth Fluorides. *Adv Chem Ser* **1968,** (72), 267-290.
62. Zmbov, K. F.; Margrave, J. L., Mass Sepctrometric Studies at High Temperatures .13. Stabilities of Samarium Europium and Gadolinium Mono- and Difluorides. *J Inorg Nucl Chem* **1967,** *29* (1), 59-63.
63. Barrow, R. F.; Chojnicki, A. H., Analysis of Optical-Spectrum of Gaseous Ytterbium Monofluoride. *J Chem Soc Farad Trans 2* **1975,** *71*, 728-735.
64. Yokozeki, A.; Menzinger, M., Molecular-Beam Chemiluminescence .8. Pressure-Dependence and Kinetics of Sm + (N_2O,O_3,F_2,Cl_2) and Yb + (O_3,F_2,Cl_2) Reactions - Dissociation-Energies of Diatomic Reaction-Products. *Chem Phys* **1976,** *14* (3), 427-439.
65. Chen, M. Y.; Dixon, D. A.; Wang, X. F.; Cho, H. G.; Andrews, L., Matrix Infrared Spectroscopic and Electronic Structure Investigations of the Lanthanide Metal Atom-Methyl Fluoride Reaction Products CH_3-LnF and CH_2-LnHF: The Formation of Single Carbon-Lanthanide Metal Bonds. *J Phys Chem A* **2011,** *115* (22), 5609-5624.
66. Hildenbrand, D. L., Dissociation-Energies of CaBr, SrBr, BaBr, and BaCl from Mass-Spectrometric Studies of Gaseous Equilibria. *J Chem Phys* **1977,** *66* (8), 3526-3529.
67. Jensen, W. B., The Positions of Lanthanum (Actinium) and Lutetium (Lawrencium) in the Periodic Table. *J Chem Educ* **1982,** *59* (8), 634-636.
68. Kramida, A.; Ralchenko, Y.; Reader, J., NIST Atomic Spectra Database, NIST Standard Reference Database 78 (https://www.nist.gov/pml/atomic-spectra-database). 2019 ed.; National Institute of Standards and Technology (NIST): Gaithersburg, MD, USA, 2019.
69. Antonov, I. O.; Barker, B. J.; Bondybey, V. E.; Heaven, M. C., Spectroscopic Characterization of Be_2^+ X^2 Σ^{+u} and the Ionization Energy of Be_2. *J Chem Phys* **2010,** *133* (7), 074309.
70. Kalemos, A., The Nature of the Chemical Bond in Be_2^+, Be_2, Be_2^-, and Be_3. *J Chem Phys* **2016,** *145* (21), 214302.
71. Solomonik, V. G.; Smirnov, A. N., Toward Chemical Accuracy in ab Initio Thermochemistry and Spectroscopy of Lanthanide Compounds: Assessing Core-Valence Correlation, Second-Order Spin-Orbit Coupling, and Higher Order Effects in Lanthanide Diatomics. *J Chem Theory Comput* **2017,** *13* (11), 5240-5254.
72. Shannon, R. D., Revised Effective Ionic-Radii and Systematic Studies of Interatomic Distances in Halides and Chalcogenides. *Acta Crystallogr A* **1976,** *32* (Sep1), 751-767.
73. Schoendorff, G.; Wilson, A. K., Low Valency in Lanthanides: A Theoretical Study of NdF and LuF. *J Chem Phys* **2014,** *140* (22), 224314-1-8.
74. Vogel, D. J.; Lee, Z. R.; Hanson, C. A.; Henkelis, S. E.; Smith, C. M.; Nenoff, T. M.; Dixon, D. A.; Rimsza, J. M., Predictive Acid Gas Adsorption in Rare Earth DOBDC Metal-Organic Frameworks via Complementary Cluster and Periodic Structure Models. *J Phys Chem C* **2020,** *124* (49), 26801-26813.
75. Kleinschmidt, P. D.; Lau, K. H.; Hildenbrand, D. L., Thermochemistry of the Gaseous Fluorides of Samarium, Europium, and Thulium. *J Chem Phys* **1981,** *74* (1), 653-660.

76. Armentrout, P. B., Guided Ion Beam Studies of Transition Metal-Ligand Thermochemistry. *Int J Mass Spectrom* **2003,** *227* (3), 289-302.
77. Cox, R. M.; Citir, M.; Armentrout, P. B.; Battey, S. R.; Peterson, K. A., Bond Energies of ThO^+ and ThC^+: A Guided Ion Beam and Quantum Chemical Investigation of the Reactions of Thorium Cation with O_2 and CO. *J Chem Phys* **2016,** *144* (18), 184309-1-15.
78. Cox, R. M.; Kafle, A.; Armentrout, P. B.; Peterson, K. A., Bond Energy of ThN^+: A Guided Ion Beam and Quantum Chemical Investigation of the Reactions of Thorium Cation with N_2 and NO. *J Chem Phys* **2019,** *151* (3), 034304.
79. Ghiassee, M.; Armentrout, P. B., Cerium Cation (Ce^+) Reactions with H_2, D_2, and HD: CeH^+ Bond Energy and Mechanistic Insights from Guided Ion Beam and Theoretical Studies. *J Phys Chem A* **2020,** *124* (13), 2560-2572.
80. Liyanage, R.; Styles, M. L.; O'Hair, R. A. J.; Armentrout, P. B., Guided Ion Beam and Ab Initio Studies of Platinum Chloride Cations. *J Phys Chem A* **2003,** *107* (48), 10303-10310.
81. Morse, M. D., Predissociation Measurements of Bond Dissociation Energies. *Accounts Chem Res* **2019,** *52* (1), 119-126.
82. Sorensen, J. J.; Tieu, E.; Sevy, A.; Merriles, D. M.; Nielson, C.; Ewigleben, J. C.; Morse, M. D., Bond Dissociation Energies of Transition Metal Oxides: CrO, MoO, RuO, and RhO. *J Chem Phys* **2020,** *153* (7), 074303.
83. Barker, B. J.; Antonov, I. O.; Heaven, M. C.; Peterson, K. A., Spectroscopic Investigations of ThF and ThF^+. *J Chem Phys* **2012,** *136* (10), 104305.
84. Evans, W. J., The Expansion of Divalent Organolanthanide Reduction Chemistry via New Molecular Divalent Complexes and Sterically Induced Reduction Reactivity of Trivalent Complexes. *J Organomet Chem* **2002,** *647* (1-2), 2-11.
85. Nief, F., Non-Classical Divalent Lanthanide Complexes. *Dalton Trans* **2010,** *39* (29), 6589-6598.
86. Kelly, R. P.; Maron, L.; Scopelliti, R.; Mazzanti, M., Reduction of a Cerium(III) Siloxide Complex To Afford a Quadruple-Decker Arene-Bridged Cerium(II) Sandwich. *Angew Chem Int Edit* **2017,** *56* (49), 15663-15666.